Original Research Article
Determination of Optical Band Gap energy of wurtzite ZnO:Ce Nanocrystallites

ABSTRACT

Aim: Determination of optical band gap energy of ZnO:Ce nanocrystallite and effect of doping on the optical band gap energy also probed.

Material and Methods: ZnO:Ce nanoparticles are synthesized by Chemical precipitation route using 1 molar solutions of Zinc Acetate and Sodium Hydroxide at 60°C. Then I molar percentage (1.72 gm) of Cerium oxide is added with the above solution and stirrered well using magnetic stirrer. Four-five drops Tri Ethyle Amine(TEA) are added as capping agent to control agglomeration. The characterization of sample was studied by XRD, FESEM, FTIR.EDAX and TEM. The UV-Vis spectrometer was used to study the Optical properties of nanopowder

Results and discussions From the XRD techniques the crystallite size of ZnO nanopowder was determined as13.83 nm at 150˚C which increased to 16.13 nm at temperatures 180˚C. FESEM showed nanoparticle of average size 13-50nm and nano clusters have size of 1μm. EDAX data is found as Zinc oxide with 99.4% and Cerium 0.6%.TEM confirm the formation ZnO:Ce nanoparticle and it has an average size about 25nm, Some nanorods with average diameter of 40 nm and length of about 290 nm were also observed. The UV absorption spectra for bulk ZnO, nanoparticles of ZnO displayed excitonic peaks at 375 nm and 369 nm respectively. The present study found absorption edge at 372 nm for ZnO:Ce nanoparticle.

Conclusion: The UV Absorption spectra showed red shift towards 372 nm due to doping with Cerium and blue shifted relative to Bulk ZnO. From the absorption spectra optical band gap is determined as 3.32 eV. It was found that energy band gap E_g decreases with doping of Ce. The analysis of optical properties shows that ZnO:Ce is promising dielectric material and has potential application in optoelectronic devices **.**

Keywords: Semi conductor, Nanomaterials, Zinc Oxide, Doping, Optical properties,

1 INTRODUCTION

Zinc Oxide , a typical II-VI compound semiconductor , with direct band gap of 3.2 eV at room temperature and 60meV as excitonic binding energy , is a very good luminescent material used in displays, UV-Vis laser, solar cell components, gas sensors and varistors [1].Zinc oxide is an excellent Ultraviolet absorber, antibacterial agent, a transparent electro conductive and piezoelectric material. ZnO has been used in solar cells, transparent electrodes, and LED's. This nanomaterial is a promising candidate for nano-electronics and photonics [1, 2]. It is a possible material to observe coherent emission without population inversion induced by Bose- Einstein condensation at the lower polariton band [3]. ZnO is more resistant to radiation and uses in the areas as piezoelectric, ferroelectric and ferromagnetic [4]. ZnO: Ce is hexagonal in symmetry with Space group $P6_{3mc}$ and Lattice parameters [2] a = 3.253 Å, b = 3.253 Å, c = 5.209 Å . The stable structure of ZnO is wurtzite [1]. A substantial effort is made on utilizing such properties in new generation of short wavelength photonic devices [4]˙In order to get better photo catalytic activity, the incorporation of rare earth ion doping is essential and that will enhance the photo current response and the separation of electron hole pairs under UV illumination [5].Since CeO2 has a band gap of ~3eV and

45 shows the fascinating properties that are similar to that of ZnO. The mixture of both materials have been
46 used for the probing of highly efficient Photo catalysis [6].The dopant sites defects induced by the doping
47 have strong impact on the structural and optical properties of Ce doped ZnO [7]. In this investigation we
48 report optical property studies of ZnO :Ce and the effect of dopant Ce ion in ZnO nanoparticle on optical
49 band gap energy.

50 **2. MATERIAL AND METHODS**

51
52 **2.1Synthesis and Characterization**

53   ZnO:Ce nanoparticles are prepared by chemical precipitation route using 1 molar solutions of Zinc
54 acetate and Sodium hydroxide at 60°C. One molar percentage (1.72 gm) of rare earth element Cerium
55 oxide solution is mixed with the above solution using magnetic stirrer. The precipitate obtained is washed
56 with double distilled water and acetone many times and filtered well. Four-five drops Tri Ethyl Amine
57 (TEA) was added as capping agent to control agglomerations. After centrifugation the precipitate
58 obtained is placed in the furnace and calcinated to 150 and 180˚C. The samples are powdered well in the
59 crucible. The X-ray diffraction spectrum of the nano powder was carried out using Rigaku DMAX
60 diffractometer with Cu -Kα radiation monochromatised with a graphite crystal. The morphology and
61 atomic percentage of elements in ZnO: Ce material was deliberated using Field Emission Scanning
62 Electron Microscopy (FESEM) and Electron Dispersive X-ray Analysis (EDAX) with a Hitachi Model s-
63 3000H Electron microscope. Fourier Transform Infrared spectroscopic (FTIR) studies was conducted
64 using Nicolet (Impact 410) FTIR Michelson interferometer..The Transmission electron microscopy (TEM)
65 was performed by JEOL 1010, TEM operating at an accelerating voltage of 100keV. Perker Elmer Lamda
66 25 UV-Vis spectrometer was used to study the Optical properties of nanopowder.

67 **3. RESULTS AND DISCUSSIONS**

68 **3.1 Determination of particle Size from XRD Pattern.**

69 The XRD pattern, Fig. 1, consists of sharp intense peaks of ZnO:Ce which confirms the good crystalline
70 nature of ZnO and peaks originated from (100), (002), (101), (102), (110), (103), (112), (201), (200) and
71 (202) reflections of hexagonal ZnO [4,5]. The XRD techniques are widely used for the particle size
72 determination and structure determination of nanoparticles. The patterns are compared with JCPDS file
73 No:80-0075 comparing the observed data with the JCPDS file. In XRD no peaks are identified to represent
74 Ce due to the small percentage of Ce incorporated into the lattice matrix of ZnS. Only a lattice strain can
75 be observed. Due to doping there will not be significant change in the structure of ZnS, whereas
76 disappearance of certain peaks and a shift in the peak position on the 2-theta scale were observed. Also
77 intensities of the peaks are decreased relate to the undoped Zinc oxide. The peaks are found to be
78 broadened. The disappearance of peaks was due to small change in crystalline structure or crystalline
79 phase. The small shift in peak position and decrease in the intensity on doping are due to change in
80 electron density or might be due to point defects. The presence of long range stain field associated with
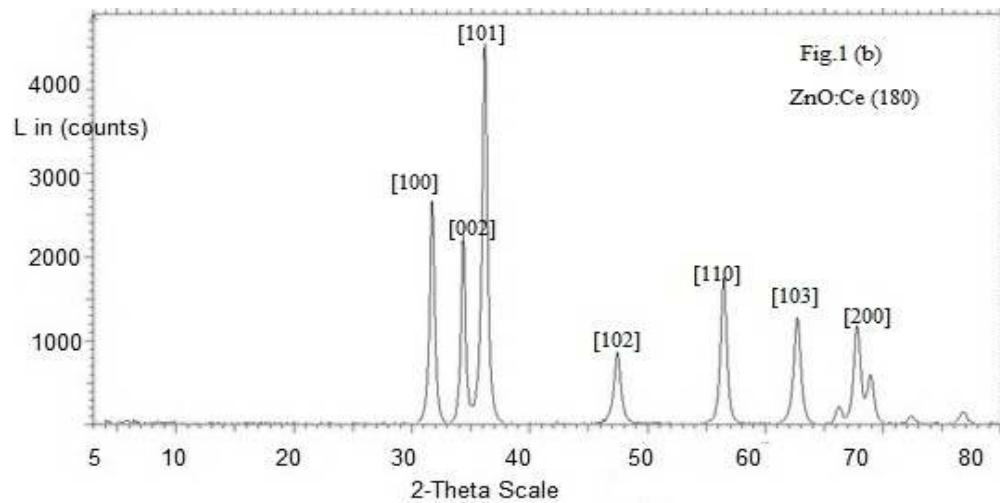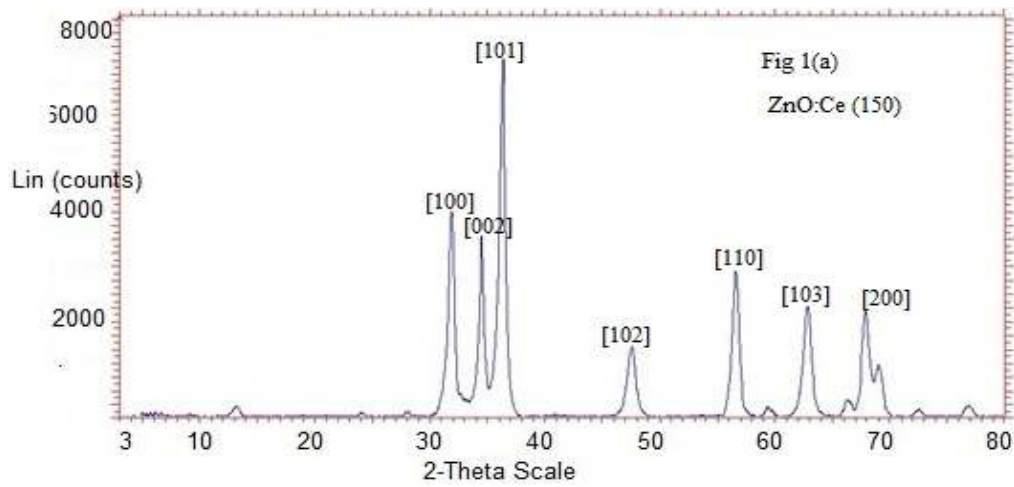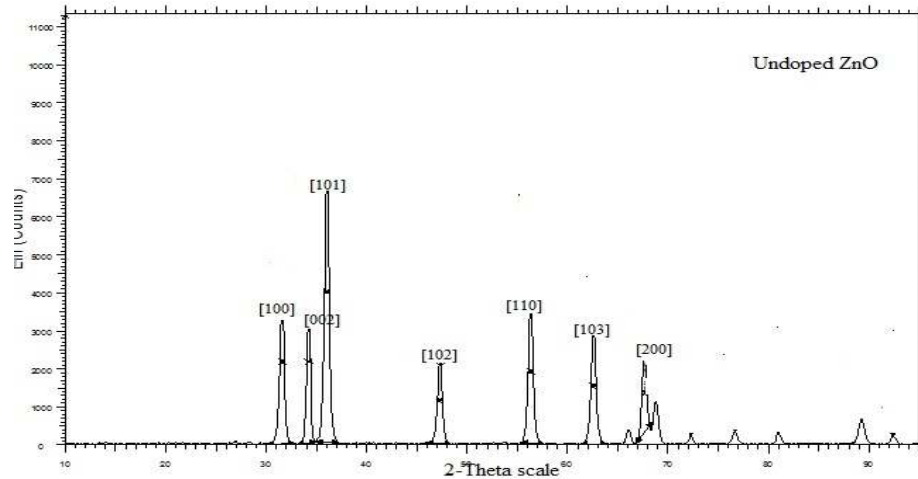81 doping causes line broadening and decrease in peak intensity

82

83

84

85

86 **Fig.1(a-b) XRD patterns of ZnO: Ce nanoparticles at 150 and 180°C.**

87 The degree of crystallinity of nanoparticles increases with annealing temperature. The percentage of
88 lattice contraction with annealing temperature can also be studied using X-ray diffraction pattern. Particle
89 Size, can be calculated by the formula [4,7], Debye- Scherrer's formula

90 $$D = K\lambda / \beta Cos\theta \qquad\qquad (1)$$

91 K= 0.89, λ the X-ray wavelength = 0.154095 nm, β the full width at half maximum and θ the half diffraction
92 angle. The crystal sizes of ZnO:Ce nano particles synthesized at 150 and 180°C were calculated from
93 FWHM and tabulated in Table 1

Table 1.Variation of Grain size of ZnO:Ce with temperature

Temperature ^{o}C	FWHM	$\beta \times 10^3$	2θ	θ	Particle size(D) nm
150	0.653	11.39	56.64	28.32	13.83
180	0.560	9.768	56.515	28.257	16.13

96 From the Fig.1(a-b) it was found that the crystallite size of ZnO nanopowder was 13.83 nm at 150°C
97 which increased to 16.13 nm at temperatures 180°C. From the above study, it is observed that there is a
98 continuous increase in the particle size with temperature. The increase in the particle size is due to the
99 amalgamation of the smaller particles into larger particles [8] is a result of solid state diffusion.

3.2 Fourier Transform Infrared Spectrum Analysis.

101 FTIR spectrum, *see* Fig. 2, of ZnO:Ce has been shown that as particle size decreases, increase in
102 frequency for the bond (blue shift) is observed in nanoparticles relative to the undoped ZnO. The
103 comparative study of Vibrational modes of doped and undoped ZnO is presented in the Table 2. The
104 stretching frequency of ZnO is observed at 489.12 cm^{-1}. Here a blue shift is observed in that frequency
105 i.e., that frequency change may be due to quantum confinement.
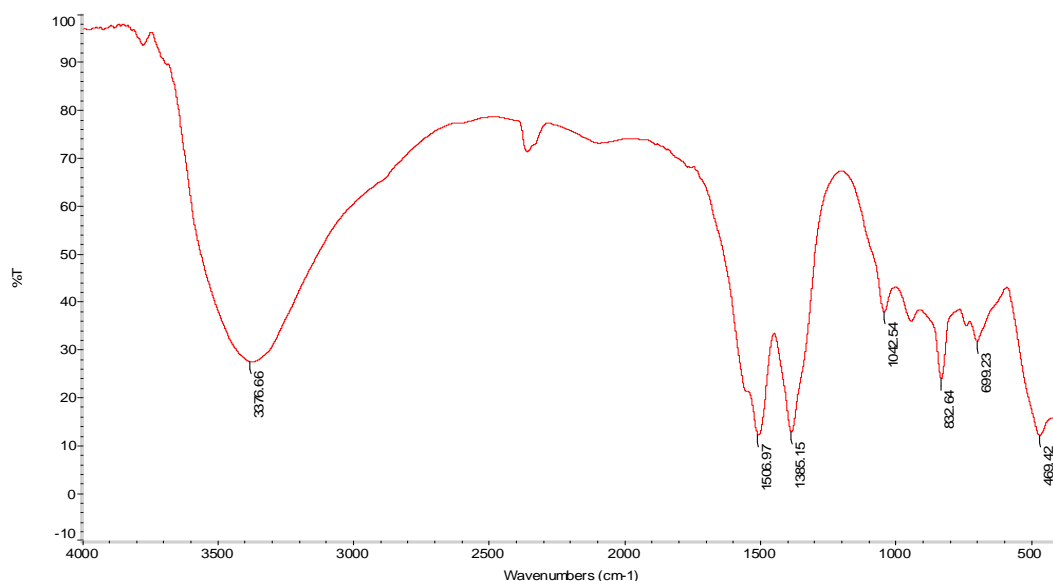
Fig.2. Fourier Transform Infrared Spectrum of ZnO: Ce nanorods

after calcination at 600°C for 4 hours

110 Three intense bands were centered at 1386.15 cm^{-1}, 1042.54 cm^{-1} and 2822 cm^{-1} and are
111 attributed to the stretching vibrations of C = O, C = C and C-H groups in acetate species, which

112 suggests its presents as absorbed species in the surface of nanoparticles. The broad absorption
113 peak centered at 3376.66 cm^{-1} and 1506.97 cm^{-1} corresponds to O-H stretching, indicating the
114 existence of water molecule occluded in the surface of nanoparticles [9] and H-O-H deformation.
115 The peak observed at 832.64 cm^{-1} and 599.23 cm-1 might be due to the presence of Ce-O
116 stretching vibration [18, 19] and Ce^{3+} doped ZnO respectively.

117 **Table 2.Comparison of Vibrational modes of undoped and Ce^{3+} doped ZnO**

118

ZnO (cm^{-1})	ZnO:Ce (cm^{-}1)	Vibrational modes
3480	3376.66	OH
2820	2822	C-H Stretching
1319	1386.15	C=O Stretching
1119.15	1506.97	HOH deformation
1050	1042.54	C=C
	832.64	Ce-O stretching vibrations
	599.23	Ce^{3+} Doped ZnO
480.27	489.12	Stretching frequency of ZnO

130

131

132

133 **3.3 Scanning Electron Microscopy (SEM).**

134 The Morphology of the nanostructure of ZnO:Ce, obtained after 4hrs of reaction, was studied using a
135 Hitachi Model s-3000H Field Emission Scanning Electron Microscope (FESEM). The orientational growth
136 of nanocrystal in water is higher [6].Spear shaped morphology is observed in the micrograph of ZnO:Ce.
137 The SEM pictures *see* Fig.3, showed distinguished self aligned prismatic and rod like morphology. The
138 Scanning Electron Microscopic image showed nanoparticles of average size 13-50 nm In SEM
139 measurement the grain size are measured. The particle size is calculated by taking the noticeable grain
140 boundaries. While in XRD, measurements are taken from the crystalline area that diffracts the X-ray
141 waves. Thus the particle size measurement of capped ZnO: Ce using XRD was found to be smaller than
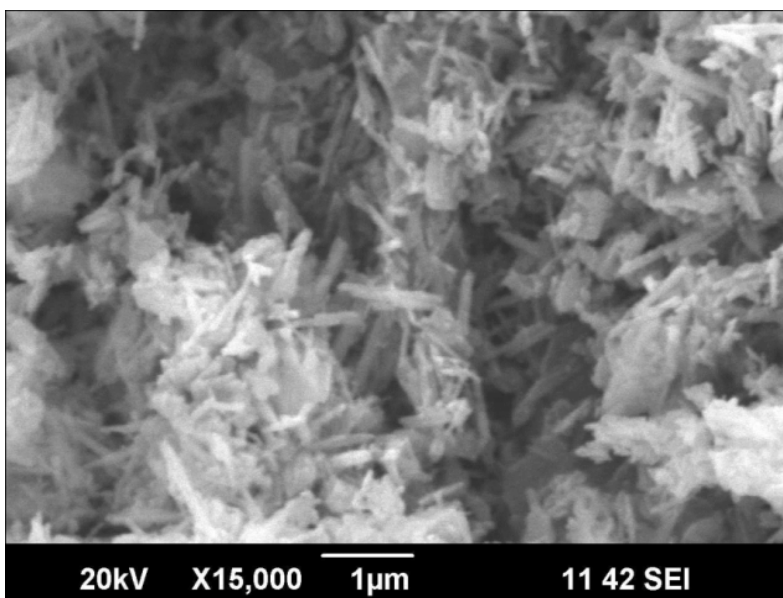142 that with SEM measurement [10].

Fig.3 SEM image of ZnO:Ce Nanorods under high magnification

3.4 Energy Dispersive Spectrum Analysis (EDAX).

EDAX is considered a relatively rapid and non destructive approach for surface analysis. Purity and composition of the sample is studied by EDAX. It is often used to survey surface analytical problems and elemental analysis. The higher a peak in a spectrum, the more concentrated the element is in the sample.
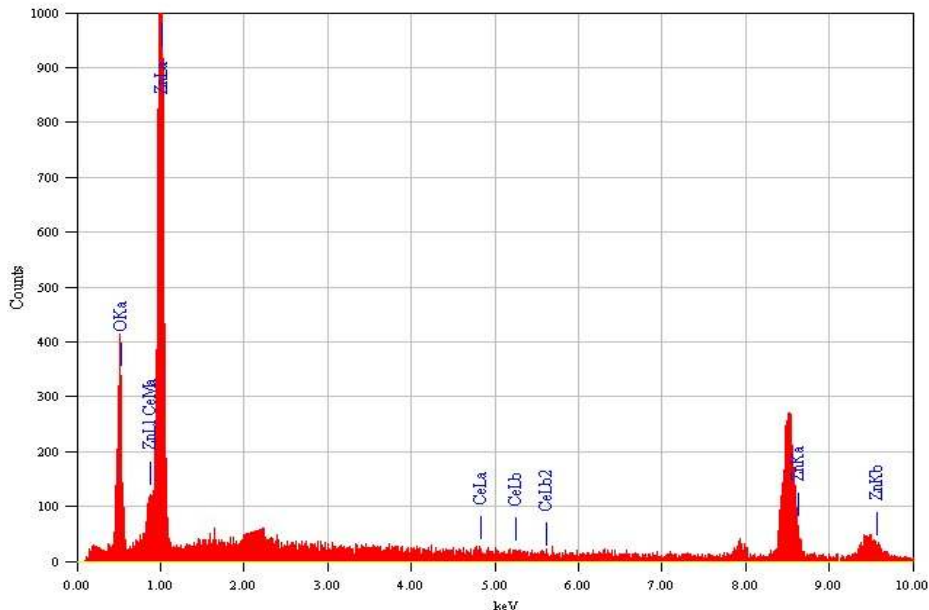

Fig 4 Energy Dispersive Spectrum of ZnO:Ce nanorods

The dried powder samples were analyzed on EDX. The observed peaks reveals the presence of Zn and O_2 confirming the formation of pure ZnO. The average atomic percentage ratio of ZnO was 43.97:56.33. A peak corresponding to the amount of energy possessed by X-rays emitted by an electron in the L-shell going down to the K-shell is identified as a K-Alpha peak. The peak corresponding to X-rays emitted by M-shell electrons going to the K-shell is identified as a K-Beta peak. High intensity peaks for Zn, O_2 and

156 minor peaks for Ce. Other peaks correspond to C and Silicate, which are due to sputter coating of glass
157 substrate on the EDX stage and were not considered in elemental analysis. The EDAX ,*see* Fig.4, of
158 ZnO:Ce nanoparticle is plotted using the recorder and The atomic percentage of elements present in the
159 sample is presented in the Table 3.The EDAX data has shown Zinc Oxide with 99.4% and Cerium 0.6%.
160 *i,e,* very small percentage was incorporated in to the ZnO matrix due to incompatible size of the impurity
161 atom.

162 **Table 3. Composition of elements in ZnO:Ce sample**

Sample	Element	Atomic percentage
	O	56.33
ZnO:Ce	Zn	43.07
	Ce	0.6

163

164 **3.5 Transmission Electron Microscopy (TEM)**

165 Fig.5 (a, b) show typical TEM Images, after 4 hours photo development, of a single ZnO:Ce nanorods to
166 confirm the crystal quality and growth direction. It is clear from TEM image that the end of the ZnO:Ce
167 nanorod is sharp tip. TEM confirm the formation ZnO:Ce nanoparticle and it has an average size about
168 25nm, Some nanorods with average diameter of 40 nm and length of about 290 nm were also
169 observed.TEM showed that the particles have nanometric prism like and rod like morphologies. The cross
170 section of the one dimensional (1D) nanostructure include triangle, hexagonal and rectangle shapes. High
171 Resolution Transmission Electron Microscopic (HRTEM) pattern indicates that the nanorods grow along
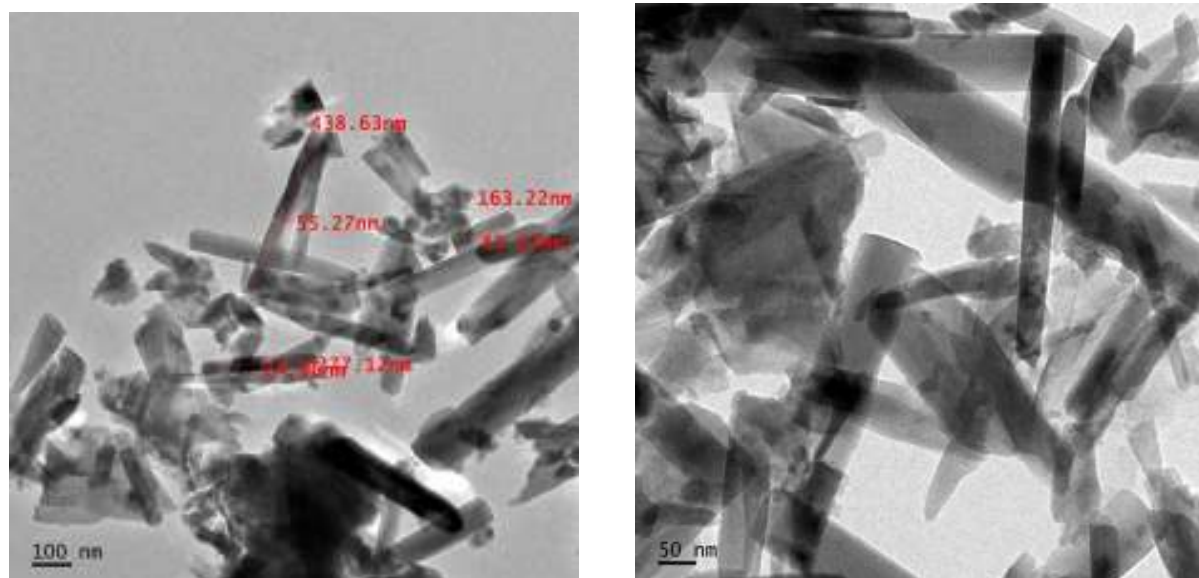172 the c-axis and it has standard hexagonal structure.

173

174 **Fig.5 (a-b) TEM images of ZnO: Ce nanorods**

175 **3.6 UV Absorption Spectra**

176 **3.6.1 Optical Band gap energy from UV absorption Spectra.**

177 Energy band gap studies of these materials have been reported using absorption spectra. The ZnO is
178 reported to be a direct band gap material [9].When an electron sitting at the bottom of the conduction
179 band recombines with a hole sitting at the top of the valence band, there will be no change in momentum
180 value. Energy is conserved in the process by emitting photon. Direct band gap materials are capable of
181 emitting photons by radiative recombination. So in order to have efficient LED's, and optoelectronic
182 devices one should choose material having direct band gap. The Fig.6 (a-b) depict the optical absorption
183 spectrum of undoped ZnO nanoparticle and ZnO:Ce nanopowder prepared under aqueous conditions. A
184 size-dependent electron-hole exchange interaction is also responsible for it and has been reported [12,
185 14]. The optical band gap energy can be computed using the relation where h, the Planck's constant, c
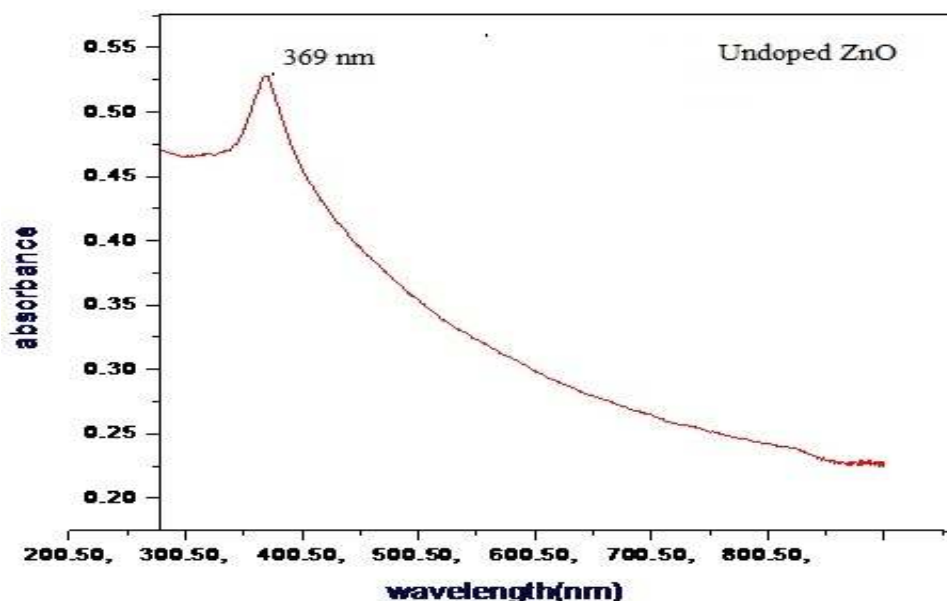186 velocity of light and λ_g wavelength corresponding to the absorption maximum.

187

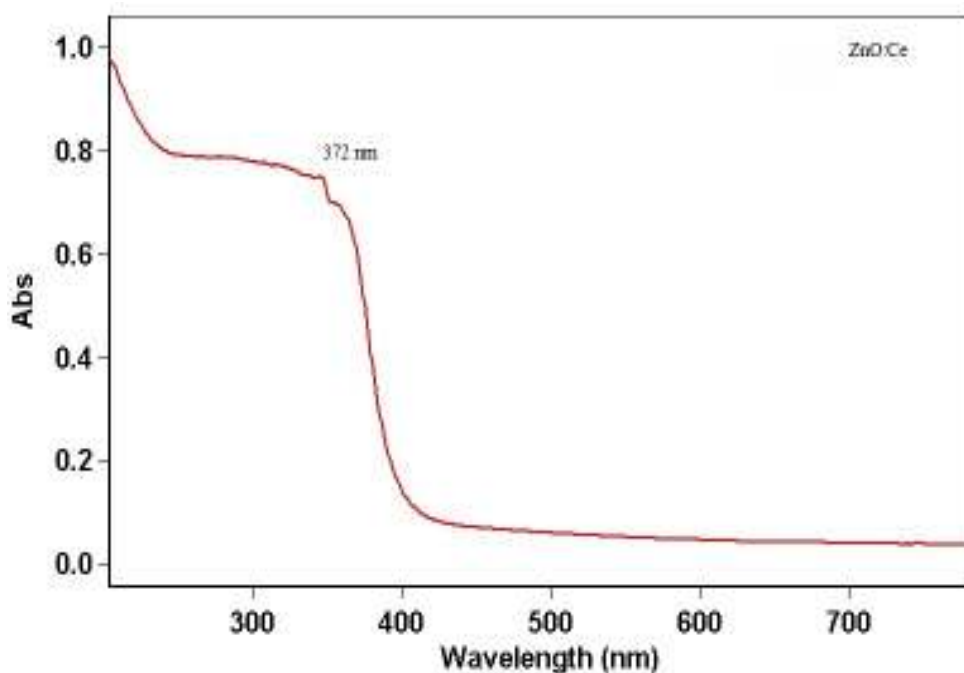188   **Fig.6(a) UV spectrum of ZnO**

189

190 **Fig 6(b) UV Spectrum of ZnO:Ce nanorods**

191

192 $$E_g = h\nu_g = hc/\lambda_g \tag{2}$$

193 The UV absorption spectra for bulk ZnO, nanocrystallite of ZnO displayed excitonic peaks at 375 nm and
194 369 nm respectively [7, 13]. The present study revealed that The UV visible spectra absorption edge is at
195 372 nm (3.32 eV) for nanocrystallite of Zinc Oxide doped with rare earth ion Cerium. The values are
196 tabulated in the Table 4. It has displayed a red shift 5 nm for absorbance. It is found that after the Ce
197 incorporation, a new localized band appears between the valence and conduction band, which
198 corresponds to the majority spin of Ce- 4f states [16]. It is this localized band constructs a bridge between
199 the valence and conduction state, which will improve the optical performance of ZnO. ZnO:Ce is a
200 degenerate semiconductor. The strong correlation effect is very important for the 4f of the Ce atom in
201 ZnO:Ce. The mismatch of the majority and minority spin of Ce-4f, Ce-5d state and the spin polarized
202 holes in O-2p state induced by Ce doping leads to the presence of magnetic order for ZnO:Ce. The
203 analysis of optical properties shows that ZnO:Ce is promising dielectric material and has potential
204 application in optoelectronic devices [15]. The introduced dopant ions might shape a shallow energy level
205 near valence band. Hence we assign the red shift to the defects and the probable shallower energy levels
206 [17]. Therefore, the optical band gap of Ce doped ZnO is broader than that of undoped Zinc Oxide. Hence
207 the value of band gap energy lies in the higher wavelength region. The changes in band gap were due to
208 the existence of a valence band-donor transition at 3.38 eV which can dominate the absorption spectrum
209 when the bulk, as distinct from the surface, of a single crystal is probed.

210 **Table 4: Band gap energy of Bulk ZnO, undoped ZnO, doped ZnO nanoparticles.**

211 **Blue/red shift observed**

Sample material	Band Gap energy E_g (eV)	Wavelength Maximum λ_{gn}(nm)	Blue shift w.r.t to bulk ZnO (eV)	Red shift w.r.t undoped ZnO nanoparticle(eV)
ZnO: Ce Nanomaterials	3.32	372	0.02	0.06
ZnO Nanomaterials	3.38	369		
ZnO Bulk material	3.3	375		

212

213 ## 4. CONCLUSIONS

214

215 The size and crystal structure of ZnO doped with Cerium was studied using XRD. The XRD results
216 indicated that the particle size of nano ZnO:Ce is much small as compared to that of pure ZnO and
217 decreases with the cerium loading. From the XRD results, it is clear that as temperature increases,
218 particle size also increases. The change in particle size cause large variation in the physical properties.
219 High temperature XRD also confirmed that the nanoparticles were stable not only at room temperature
220 but at high temperature as well. The UV Absorption spectra showed red shift towards 372 nm due to
221 doping with Cerium. From the absorption spectra obtained by UV-Vis spectrometer the   optical band gap
222 is determined and found to be in the range 3.32 eV. It was found that energy band gap E_g decreases with
223 doping of Ce. Doping of Ce changed the free carrier concentration in the ZnO nanoparticles. The analysis
224 of optical properties shows that ZnO: Ce is promising dielectric material and has potential application in
225 optoelectronic devices.

226

REFERENCES

1   Karpina VA., Crys.Res.Tech, 2004; 39; 980.

2   Bernal R, Cruz VC, Optical Materials, 2005; 27 12; 35.

3   Imamoglu R J, Yamamoto Y, Phys.Rev A ,1996; 53; 4250.

4   Kumbhakar P, Singh D, Chalcogenide Letters, 2008; 5; 387.

5   Liu TX,Li XZ, Li FB, Chemical Engineering Journal, 2010; 157(2-3);475

6   Li GR, Lu XH, Lu XW, Zhao X, Tang YX, Crystal growth Design, 2008; 8(2);1276.

7   Yang JH, Gao M,Wang YX, Fan HG, Applied Surface Science, 2008; 255 (5); 2646.

8   Nanda K K, Kruis F E, Hassan H, Phys.Rev.Lett. 2002; 89; 256103.

9   Xu, Love, L C, Wolfe D B, Whitesides G M, Annu.Rev.Mater.Res. 2004;34;339.

10   Shashi B Rana,Amarpal Singh, Electronic Material Letters,2014,13,(In press)

11   Srikant V, Clarke D R, J.Appl.Phys, 1998; 83; 5447.

12   Chang HJ,Cheng ZL ,J of Korean Physical Society, 2004; 45(4);959.

13   Soosan S, Lekshmi B, SB Academic Review, 2009;1-2; 57.

14   Tingting Ren, Holly RB, Thin Solid Films, 2007; 515; 7976.

15   Iqbal J, Liu XF, Zhu XC ,Yu RH, J.Appl. Phys. 2009;106; 835115.

16   Ali Fathima A, Suganthi Devadason, J Pure Applied & Industrial Physics, 2011; 1 (2); 115-120.

17   Nadia Febiana, Djaja,Roseri, Saleh, Mat. Sci & Applications, 2013; 4; 145-152.

18   Harish Kumar, Rani R., Int. Letts. of Chem. Phys, Chem. and Astronomy, 2013; 14; 26-36

19.   Sudheesh K S,.Agorku E.S, Chem. Papers DOI:10.2478/s11696-013-0442-5